RSC Advances

RSC Publishing

PAPER

Effect of metal ions (Li^+, Na^+, K^+, Mg^{2+} and Ca^{2+}) and water on the conformational changes of glycosidic bonds in heparin oligosaccharides†

Cite this: *RSC Advances*, 2013, **3**, 9843

Milan Remko,*[ab] Piet Th. Van Duijnen[c] and Ria Broer[c]

The effects of complexation by Li^+, Na^+, K^+, Mg^{2+}, and Ca^{2+} counterions and water on the molecular structure of the Fondaparinux pentameter (D–E–F–G–H) and its dimer units (D–E, E–F, F–G and G–H) are studied using Becke 3LYP hybrid density functional theory and molecular modeling. The ionic charge state, the number of metal ion adducts and the counterion radii are important factors that influence counterion-induced conformational changes in these pentamers and dimers of heparin. The displacement of the Li^+, Na^+, K^+, Mg^{2+} and Ca^{2+} cations from their binding sites in the salts results in appreciable changes in the anion conformations. The interaction energies are very negative and span a broad range from −1900 to −16 000 kJ mol^{-1}, which is the result of multiple coordinate bonds between ions and basic centers in glycosaminoglycan units.

Received 1st February 2013,
Accepted 9th April 2013

DOI: 10.1039/c3ra40566d

www.rsc.org/advances

Introduction

Heparin is a complex saccharide that resides in extracellular environments and contributes to a number of pathological and physiological processes, such as anticoagulation, growth factor control, hemostasis, and cell adhesion.[1–5] Heparin is a structurally heterogeneous sulfated copolymer composed of repeating 1 → 4 linked disaccharide subunits containing either uronic acid or glucuronic acid and glucosamine residues.[5–7] These residues are substituted with *N*- or *O*-sulfate groups to various degrees. Heparin is strongly acidic because it contains covalently linked sulfate and carboxylic acid groups. Because of its highly acidic sulfate and carboxylate groups,[8,9] heparin exists as an anion at physiological pH values. The heparin polyanion is one of the most acidic species of natural origin, and it binds to active sites on proteins.[10] Heparin was discovered in 1916 as an anticoagulant, and it has been used in clinical applications since 1935. Its antithrombotic activity is attributed to its interactions with the protein antithrombin III (AT–III).[7,10,11] Heparin anticoagulants bind to antithrombin through a group of five subunits (D–E–F–G–H), a unique pentasaccharide fragment (PS) that constitutes the minimal binding domain for AT–III.[10,11] The preparation of PS and its many analogues led to the identification of the structure – activity relationships of heparin-like pentasaccharides.[10,13] Despite its importance, the experimental 3D molecular structures of heparin and its lower molecular weight derivatives are unknown. Likewise, the structures of glycosaminoglycans have not been characterized, despite their interesting properties. The absence of experimental structural data for the basic structural units of the glycosaminoglycans presents a challenge to the application of molecular modeling to gain insight into the recognition and binding processes. The molecular structure and properties of the dimeric (D–E, E–F, F–G, and G–H), trimeric (D–E–F and F–G–H) and pentameric (D–E–F–G–H) structural units of the pentasaccharide Fondaparinux were examined theoretically using density functional theory.[12–15] The effect of counterions Na^+ and Ca^{2+} and water on the conformational structure of heparin disaccharide containing induronic acid residue using a hybrid quantum mechanical/molecular mechanical method was studied quite recently.[16]

Heparin forms complexes with cations, especially alkaline-earth and multivalent cations.[17–19] However, the mechanism of these interactions is controversial, particularly for bivalent cations.[20–22] The interaction of Na^+, Mg^{2+}, Ca^{2+}, Zn^{2+} and La^{3+} with heparin was studied by nuclear magnetic spectroscopy and discussed in the terms of heparin – metal binding constants.[23] The effect of Na^+ ions on the heparin – protein interaction was also examined.[24] However, to our knowledge, there is no systematic theoretical and/or experimental study of the effect of alkali and alkali earth metal cations on the conformational structure of glycosidic bonds in the unique pentasaccharidic (D–E–F–G–H) structural unit of heparin. The present paper reports detailed structural parameters for four

[a]*Department of Pharmaceutical Chemistry, Comenius University in Bratislava, Odbojarov 10, SK-832 32 Bratislava, Slovakia. E-mail: remko@fpharm.uniba.sk*
[b]*Center for Hemostasis and Thrombosis, Hemo Medika Bratislava, Šustekova 2, 851 04 Bratislava, Slovakia*
[c]*Department of Theoretical Chemistry, Zernike Institute for Advanced Materials, University of Groningen, Nijenborgh 4, 9747 AG Groningen, The Netherlands*
† Electronic supplementary information (ESI) available. See DOI: 10.1039/c3ra40566d

disaccharides (D–E, E–F, F–G, and G–H) and the pentasaccharide (D–E–F–G–H) Fondaparinux. The conformations defined by rotations around glycosidic bonds in the oligomeric species of heparin and the effects of metal ions, metal affinities and solvent effect are of particular interest. The results of theoretical studies of these species were compared with the available experimental data and discussed relative to the current mechanistic theories.

Computational details

The geometries of the Li^+, Na^+, K^+, Mg^{2+} and Ca^{2+} salts of the heparin structural units D–E, E–F, F–G, G–H and D–E–F–G–H (Fig. 1) have been completely optimized with the Gaussian 09 program system[25] using the density functional theory (DFT)[26–28] and the Becke 3LYP[29–31] theory with the 6-31G(d) and B3LYP/6-311+G(d,p) basis sets.[32] To check the correctness of the relative energies calculated with B3LYP using the double-ζ basis set, we also performed calculations for the dimers using a basis set of triple-ζ quality (B3LYP/6-311+G(d,p) level of theory). The interaction energy, ΔE, for the reaction of a cation with a Lewis base $[M^{n+}(g) + L^{-}(g) \rightarrow M^{n+}\cdots L(g)]$ (M^{n+} = Li^+, Na^+, K^+, Mg^{2+} and Ca^{2+}) is given by the following equation:

$$\Delta E = E(M^{n+}\cdots\text{Ligand}) - \{E(M^{n+}) + E(\text{Ligand})\} \quad (1)$$

where $E(M^{n+})$ and E(Ligand) are the energies of the metal cation and ligand molecules, respectively, and $E(M^{n+}\cdots\text{Ligand})$ is the energy of the complex. The solvation energies of the neutral and anionic species in aqueous solution were computed using the CPCM solvation method.[33–36] All gas phase and condensed phase (CPCM) structures were fully optimized without geometric constraints.

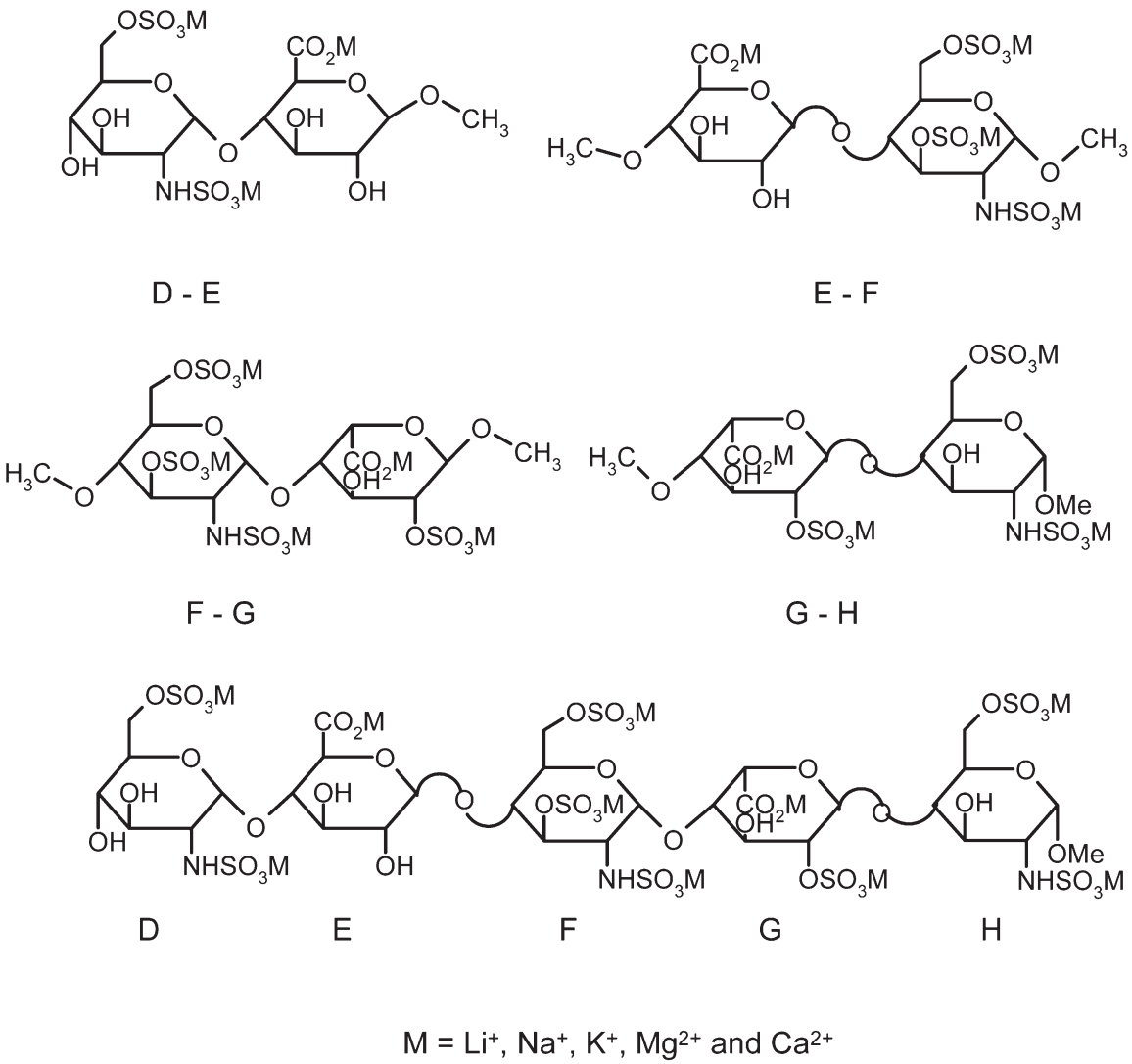

Fig. 1 Structure of the heparin species investigated.

Results and discussion

General considerations

Heparin is a highly charged, sulfated polysaccharide composed of repeating disaccharide units. The twenty-four disaccharides that can be formed from the basic monosaccharides are the fundamental sequence units of heparin.[5] Of these disaccharides, IndoA(2*S*)−(1 → 4)GlcNS(6*S*) (dimer G–H, Fig. 1) is the most abundant in heparin. In this study, we investigated the D–E, E–F, F–G and G–H disaccharides in heparin's unique antithrombin-binding pentasaccharide sequence D–E–F–G–H in which two neighboring monomers bound by (1–4) glycosidic bonds are substituted with methyl groups (Fig. 1). It was assumed that the pyranose rings of the D-glucosamine in these dimers had relatively stable $^4C_1$ conformations. The observations of L-iduronic acid, the structural unit G in the dimers F–G and G–H, in the more stable skew-boat ^2S_o form were applied.[5,9,37]

Initial conformations for the DFT calculations of the metal complexes of the dimers and the pentamer were based on published molecular structures of the free acids of these oligomers.[14] Suitable starting geometries for lithium, sodium, potassium, magnesium and calcium salts were generated from the geometries of the corresponding acids (Fig. 1). The initial calculations were carried out using the B3LYP/6-31G(d) method. The initial optimization was performed at the lower level of this theory to shorten the calculation times and provide better starting structures for the higher level calculations. The effect of the basis set extension (to the triple-ζ quality 6-311+G(d,p) basis) on the species geometries was also investigated. The extension of the basis set in the DFT calculations resulted in only small changes in the equilibrium geometry of the dimer metal complexes. The dihedral angles of the glycosidic bonds were optimized using two basis sets within the DFT theory, and most results agreed to within 2–5° (Tables 1–5). The relative insensitivity of the geometry optimization calculations to the density functional method was observed for diverse sets of drugs.[38,39] Therefore, the B3LYP/6-31G(d) model chemistry is a preferred method for determining reasonable geometries of larger heparin oligomers.

The effect of bulk solvent was treated with the CPCM (conductor-like polarizable model).[33–36] Water has an important effect on the geometry of the glycoside bonds in the metal complexes (Tables 1–5). The effect of water is illustrated for the (D–E–F–G–H)·K^+ pentamer in Fig. 2. For hydrated geometry optimizations, the solvation energy is computed as the difference between the energies of the optimized gas phase structure and the solvated structure that was optimized in aqueous solution. Table 6 contains water stabilization energies from CPCM calculations and dipole moments for geometries that were fully optimized *in vacuo*. The charge complexes containing Mg^{2+} and Ca^{2+} cations with a formal positive charge of +1 are most stable in water as expected because their dipole moments are significant. The computed solvation energies for neutral complexes containing alkali metal ions are substantially lower (Table 6). The solvation energy stabilization of the anions is approximately 800–7200 kJ mol^{-1} higher than the neutral complexes. This trend correlates well with the degree of ionization of the individual oligomers and indicates considerable stabilization of the pentameric anionic species of Fondaparinux in aqueous solution (Table 6). The conductor-like polarizable continuum model CPCM is one of the most successful solvation models.[40] It has been shown previously that this method reproduces hydration energies with accuracy of a few kcal mol^{-1} but mostly even better than 1 kcal mol^{-1}.[41]

Geometry of dimeric and pentameric M^{n+} (M^{n+} = Li^+, Na^+, K^+, Mg^{2+} and Ca^{2+}) complexes

The shapes of the Li^+, Na^+, K^+, Mg^{2+} and Ca^{2+} salts of the dimeric and pentameric structural units of heparin are shown in Fig. 1A–5A, ESI.† The optimized structure of the free acid of the D–E dimer is stabilized by means of system of intramo-

Table 1 Optimized glycosidic bonds (Å), bond angles (°) and torsion angles (°) of the complexes dimer (D–E)·M^{n+} (M^{n+} = Li^+, Na^+, K^+, Mg^{2+} and Ca^{2+})

Complex D–E	Φ	Ψ	C(1)–O	O–C(4′)	τ	Φ_H	Ψ_H
Li(I) salt							
B3LYP/6-31g(d)	58.8	−154.5	1.416	1.414	120.8	−58.8	−35.8
B3LYP/6-31g(d)–CPCM	50.8	−156.5	1.416	1.424	120.6	−67.3	−38.6
B3LYP/6-311+g(d,p)	60.6	−156.5	1.413	1.415	121.1	−56.9	−38.2
Na(I) salt							
B3LYP/6-31g(d)	57.0	−157.5	1.412	1.419	120.5	−59.8	−39.6
B3LYP/6-31g(d)–CPCM	56.7	−159.2	1.411	1.424	119.2	−60.3	−41.6
B3LYP/6-311+g(d,p)	60.5	−161.7	1.408	1.421	120.8	−56.4	−44.2
K(I) salt							
B3LYP/6-31g(d)	59.2	−163.9	1.405	1.423	119.9	−62.2	−46.9
B3LYP/6-31g(d)–CPCM	55.2	−160.5	1.410	1.427	118.8	−61.4	−43.4
B3LYP/6-311+g(d,p)	61.7	−165.9	1.405	1.424	120.1	−55.0	−48.7
Mg(II) salt							
B3LYP/6-31g(d)	56.4	−149.3	1.422	1.423	121.1	−61.0	−29.6
B3LYP/6-31g(d)–CPCM	59.0	−154.3	1.416	1.415	120.4	−59.0	−35.3
B3LYP/6-311+g(d,p)	56.3	−148.1	1.421	1.426	120.3	−60.0	−28.9
Ca(II) salt							
B3LYP/6-31g(d)	52.6	−152.1	1.417	1.421	121.0	−64.5	−32.8
B3LYP/6-31g(d)–CPCM	55.7	−156.5	1.417	1.421	118.7	−61.3	−38.0
B3LYP/6-311+g(d,p)	67.4	−164.4	1.410	1.423	122.4	−50.7	−45.9

Table 2 Optimized glycosidic bonds (Å), bond angles (°) and torsion angles (°) of the complexes dimer (E–F)·M^{n+} (M^{n+} = Li^+, Na^+, K^+, Mg^{2+} and Ca^{2+})

Complex dimer E–F	Φ	Ψ	C(1)–O	O–C(4′)	τ	Φ_H	Ψ_H
Li(I) salt							
B3LYP/6-31g(d)	−68.1	−101.9	1.382	1.461	114.4	49.6	15.3
B3LYP/6(31g(d) (CPCM	−84.6	−98.6	1.391	1.438	91.7	34.8	22.1
B3LYP/6(311+g(d,p)	−68.6	−102.9	1.381	1.463	114.2	48.9	14.3
Na(I) salt							
B3LYP/6(31g(d)	−9.2	−139.3	1.440	1.421	120.7	110.1	−20.0
B3LYP/6-31g(d)–CPCM	−38.1	−118.0	1.415	1.428	116.1	81.7	0.9
B3LYP/6-311+g(d,p)	−55.8	−85.3	1.417	1.428	117.3	60.2	37.8
K(I) salt							
B3LYP/6-31g(d)	40.2	−142.6	1.414	1.426	123.5	155.6	−25.5
B3LYP/6-31g(d)–CPCM	35.7	−133.6	1.425	1.427	122.3	151.4	−15.7
B3LYP/6-311+g(d,p)	36.9	−143.5	1.413	1.426	123.9	152.5	−26.3
Mg(II) salt							
B3LYP/6-31g(d)	−52.5	−108.3	1.397	1.425	112.7	62.9	10.6
B3LYP/6-31g(d)–CPCM	−56.5	−94.3	1.411	1.426	116.2	59.5	27.5
B3LYP/6-311+g(d,p)	−51.3	−79.1	1.563	1.490	108.3	64.1	40.1
Ca(II) salt							
B3LYP/6-31g(d)	−65.9	−94.7	1.467	1.478	109.6	48.3	26.7
B3LYP/6-31g(d)–CPCM	−68.9	−89.0	1.417	1.429	114.4	47.2	32.8
B3LYP/6-311+g(d,p)	−65.2	−93.8	1.475	1.480	109.6	49.1	27.5

lecular hydrogen bonds between hydroxyl groups and neighboring proton acceptors.[14] The dimer conformation is stabilized by internal hydrogen bonding between the C(2)–$NHOSO_3H$ group on the ring in the D monosaccharide and the proton-accepting C(3′)OH group in the E monosaccharide. In contrast, for metal complexes of this dimer, one metal cation symmetrically bridges two oxygen atoms in the C(5)–OSO_3 M^{n+} (M^{n+} = Li^+, Na^+, K^+, Mg^{2+} and Ca^{2+}) group. Two metal cations are involved in two tridentate coordination bonds that stabilize the conformation of the glycoside linkage. One metal cation in the C(2)–$NHSO_3M^{n+}$ group coordinates with one oxygen atom in the C(3′)OH group. The third metal cation forms an almost symmetric bridge between the two oxygen atoms in the C(5′)–$COOM^{n+}$ group and the oxygen atom in the C(4)OH group (Fig. 1A, ESI†). The equilibrium distances $M^{n+}\cdots O$ decrease in the following order: $K^+ > Ca^{2+} \geqslant Na^+ > Mg^{2+} \geqslant Li^+$, which correlates well with the general trends observed for other biologically important metal complexes.[42] Molecular superimposition of the metal salts of this dimer shows that, upon metal cation coordination, the largest conformational changes occur for the flexible *N*-sulfated and *O*-sulfated groups in structural unit D (Fig. 3).

Subunit F in the E–F dimer is substituted with three sulfate groups. In metal complexes, these sulfate groups participate in multiple bonds that form bridges between internal anionic groups and metal cations in unique equilibrium structures (Fig. 2A, ESI†). In addition, the structure of the monosaccharide F is stabilized by the system of coordinate metal bonds formed between the metal cations and the anionic sulfate groups. Alkaline metal cations bind to this dimer in a similar

Table 3 Optimized glycosidic bonds (Å), bond angles (°) and torsion angles (°) of the complexes dimer (F–G)·M^{n+} (M^{n+} = Li^+, Na^+, K^+, Mg^{2+} and Ca^{2+})

Complex dimer F–G	Φ	Ψ	C(1)–O	O–C(4′)	τ	Φ_H	Ψ_H
Li(I) salt							
B3LYP/6–31g(d)	63.1	−150.1	1.415	1.429	119.7	−54.9	−30.5
B3LYP/6-31g(d)–CPCM	58.5	−144.3	1.417	1.427	119.8	−59.4	−24.5
B3LYP/6-311+g(d,p)	63.8	−150.2	1.416	1.429	120.4	−54.3	−30.7
Na(I) salt							
B3LYP/6-31g(d)	93.9	−158.4	1.425	1.416	123.3	−24.9	−38.3
B3LYP/6-31g(d)–CPCM	93.8	−170.4	1.410	1.430	122.5	−24.3	−50.9
B3LYP/6-311+g(d,p)	92.8	−157.5	1.426	1.418	122.9	−25.4	−37.7
K(I) salt							
B3LYP/6-31g(d)	84.4	−155.8	1.420	1.430	120.1	−33.7	−35.4
B3LYP/6-31g(d)–CPCM	73.4	−153.9	1.416	1.439	118.5	−44.3	−33.9
B3LYP/6-311+g(d,p)	84.9	−157.5	1.406	1.437	120.0	−33.4	−37.6
Mg(II) salt							
B3LYP/6-31g(d)	57.2	−147.6	1.411	1.455	121.5	−63.7	−26.9
B3LYP/6-31g(d)–CPCM	60.5	−155.1	1.415	1.433	121.3	−59.7	−35.2
B3LYP/6-311+g(d,p)	57.4	−147.9	1.411	1.457	121.8	−63.2	−27.4
Ca(II) salt							
B3LYP/6-31g(d)	59.5	−148.4	1.409	1.451	120.1	−60.6	−28.0
B3LYP/6-31g(d)–CPCM	61.4	−157.5	1.413	1.431	120.0	−57.9	−37.9
B3LYP/6-311+g(d,p)	59.2	−149.4	1.410	1.451	120.9	−60.8	−29.1

Table 4 Optimized glycosidic bonds (Å), bond angles (°) and torsion angles (°) of the complexes dimer (G–H)·M^{n+} (M^{n+} = Li^+, Na^+, K^+, Mg^{2+} and Ca^{2+})

Complex dimer G–H	Φ	Ψ	C(1)–O	O–C(4′)	τ	Φ_H	Ψ_H
Li(I) salt							
B3LYP/6-31g(d)	−39.0	−108.1	1.478	1.441	115.2	77.4	10.4
B3LYP/6(31g(d) (CPCM	−36.8	−108.5	1.448	1.443	116.2	80.1	10.8
B3LYP/6-311+g(d,p)	−38.0	−109.1	1.481	1.441	115.2	78.4	9.5
Na(I) salt							
B3LYP/6-31g(d)	−57.9	−129.2	1.469	1.446	114.4	59.5	−11.9
B3LYP/6-31g(d)–CPCM	−61.8	−128.8	1.429	1.435	115.8	56.0	−9.8
B3LYP/6-311+g(d,p)	−56.9	−129.8	1.474	1.447	114.6	60.6	−12.7
K(I) salt							
B3LYP/6-31g(d)	−63.8	−124.2	1.419	1.433	116.1	54.4	−6.7
B3LYP/6-31g(d)–CPCM	−65.6	−124.3	1.422	1.430	116.6	52.6	−5.4
B3LYP/6-311+g(d,p)	−63.9	−124.8	1.422	1.434	116.3	54.3	−7.3
Mg(II) salt							
B3LYP/6-31g(d)	−49.2	−104.7	1.553	1.494	110.4	64.1	10.9
B3LYP/6-31g(d)–CPCM	−24.6	−107.9	1.472	1.449	115.7	91.5	8.3
B3LYP/6-311+g(d,p)	−42.8	−88.7	1.461	1.433	113.6	73.4	29.9
Ca(II) salt							
B3LYP/6-31g(d)	−47.8	−84.8	1.447	1.440	114.3	68.5	34.2
B3LYP/6-31g(d)–CPCM	−48.0	−85.3	1.421	1.441	114.4	69.1	33.6
B3LYP/6-311+g(d,p)	−46.3	−85.5	1.454	1.439	113.9	70.1	33.8

way. However, the coordination of bivalent cations Mg^{2+} and Ca^{2+} to the E–F dimer produces a larger conformational rearrangement of this saccharide (Fig. 2A, ESI†).

Dimer F–G is substituted with five sulfate and carboxylate groups and is the most highly sulfated dimeric residue in heparin, which is a penta-anion in its ionized state. Equilibrium conformations of metal complexes of this dimer are stabilized by multiple coordinate bonds between five metal cations and highly basic *O*-sulfated, *N*-sulfated and carboxylate groups. Individual metal cations coordinate differently to this structure (Fig. 3A, ESI†). All cations except calcium in the C(6′)–OSO_3M^{n+} moiety are bound by symmetric bifurcated coordinate bonds with optimal $M^{n+}\cdots O$ lengths (M^{n+} = Li^+, Na^+, Mg^{2+} and Ca^{2+}) of 1.88, 2.23, 1.98 and 2.24 Å, respectively. The other four sulfate and carboxyl groups form multicoordinate bonds *via* their corresponding cations with electronegative oxygen atoms in the neighboring groups (Fig. 3A, ESI†).

The cations in the optimized (G–H)·M^{n+} (M^{n+} = Li^+, Na^+, K^+, Mg^{2+} and Ca^{2+}) complexes always coordinate with two polar groups in neighboring pyranose rings (Fig. 4A, ESI†). The monovalent alkali metal ions always coordinate with two neighboring polar groups of this dimer. Optimal $M^+\cdots O$ (M^{n+} = Li^+, Na^+ and K^+) distances decrease in the following order: $K^+ > Na^+ > Li^+$, and they correlate approximately with the ionic radii for Li^+ (0.6 Å), Na^+ (0.95 Å), and K^+ (1.33 Å), respectively.[43,44] Different conformations occur with Mg^{2+} and Ca^{2+} salts. These cations in the C(2′)–$NHSO_3M^{n+}$ moiety participate in symmetric bifurcated coordination bonds with optimal $M^{n+}\cdots O$ lengths (M^{n+} = Mg^{2+} and Ca^{2+}) of 2.04 and 2.28 Å, respectively (Fig. 4A, ESI†).

The geometry of the optimized Li^+, Na^+, K^+, Mg^{2+} and Ca^{2+} salts in the D–E–F–G–H pentameric complexes is shown in the Supporting Information (Fig. 5A, ESI†). In the free acid of Fondaparinux, ten acidic sulfate and carboxyl groups participate in a network of intramolecular hydrogen bonds that stabilizes the pentasaccharide chain in a ''bent'' conformation.[14] For the metal complexes of this pentasaccharide, the formation of multiple coordination bonds by ten monovalent and bivalent cations with the pentasaccharide substituents is characteristic. The affinity of metal cations for polyanionic species such as heparin oligomers is affected strongly by the geometric features of the coordination sites, stereoisomer effects, the type of coordination, and the type and character of the non-covalent interactions at or near the monomer binding groups.[10,13] Site binding, which involves specific ''adjacent'' carboxylate, *N*- and *O*-sulfate anions–cation complexes, was observed in simple salts of the CH_3CO_2M, CH_3OSO_3M and CH_3NHSO_3M (M = Li^+ and Na^+) complexes, and site binding leads to the formation of ''bifurcated'' structures.[45] In more complex oligomeric structural units of heparin, carboxylate, *N*- and *O*-sulfate anionic groups participate in nonspecific tri- or tetradentate coordination with the metal cations (Fig. 5A, ESI†). In the favorable pentasaccharide-M_{10} complexes (M = Li^+, Na^+, K^+, Mg^{2+} and Ca^{2+}), the D, E, F, G and H pyranose rings are in positions that permit tri- or tetradentate metal coordination. One exception is the C(5)OSO_3M^{n+} (M^{n+} = Li^+, Na^+, K^+, Mg^{2+} and Ca^{2+}) moiety of the non-reducing D end of the pentasaccharide. This moiety is oriented outward along the radius of interaction with the polar substituents on the pyranose D ring, where the M^{n+} atom forms a bifurcated coordinate bond with the sulfate group. The non-reducing D–E–F end of the pentasaccharide is crucial for its initial binding to antithrombin, and the reducing end of the G–H dimer is responsible for the final stabilization of this interaction.[46] This pentasaccharide contains five *O*-sulfate groups, three *N*-sulfate groups and two carboxylate moieties, which coordinate with the ten metal cations. In the antithrombin–pentasaccharide complex, these acidic groups ionize completely and interact with the complementary (Arg, Lys, Glu and Asn) side chains on the protein.[11,47] Therefore, it is probable that the C(5)OSO_3^- group of the non-reducing structural unit is, for stereochemical reasons, a primary anchoring group of heparin drugs in

Table 5 B3LYP/6-31G(d) optimized glycosidic torsion angles (°) of the complexes pentamer (D–E–F–G–H)·M^{n+} (M^{n+} = Li^+, Na^+, K^+, Mg^{2+} and Ca^{2+})

	D–E–F–G–H, calculation													D–E–F–G–H, experiment[a]			
Glycosidic angle (°)	H (acid)	Solvated H acid	Li salt	Solvated Li salt	Na salt	Solvated Na salt	K salt	Solvated K salt	Mg salt	Solvated Mg salt	Ca salt	Solvated Ca salt	Anion	Solvated anion	1AZX[b]	1E03[b]	1NQ9[c]	2GD4[d]
Φ_1	76.7	77.4	64.0	56.8	63.7	48.3	63.9	51.0	53.5	61.3	64.6	58.1	66.1	59.5	89.3 (91.0)	84.7 (96.9)	81.5 (77.7)	101.4
Ψ_1	167.3	166.3	−164.5	−160.8	−169.8	−155.5	−176.4	−162.3	−152.8	−163.6	−164.4	−165.7	−158.3	−164.5	−141.4 (−154.1)	−137.0 (−153.7)	−137.6 (−142.6)	−157.6
Φ_2	−105.3	−106.0	−119.7	−116.4	−124.8	−101.9	−120.6	−102.9	−91.1	−84.6	−94.8	−81.9	−86.8	−97.8	−86.0 (−79.6)	−87.3 (−72.4)	−89.0 (−86.5)	−84.4
Ψ_2	−93.0	−94.5	−66.5	−68.3	−77.7	−76.7	−73.4	−82.9	−77.5	−86.8	−82.2	−89.1	−92.3	−80.4	−112.7 (−118.8)	−112.5 (−116.8)	−108.6 (−107.4)	−120.8
Φ_3	72.4	69.2	53.9	45.6	54.3	54.2	54.5	64.1	58.5	48.2	54.7	51.6	77.2	69.9	55.4 (49.1)	58.7 (45.7)	59.2 (58.4)	63.1
Ψ_3	−148.7	−148.9	−168.9	−170.0	−175.9	−168.1	−173.7	−165.2	−168.4	−164.0	−171.8	−171.1	−152.4	−153.0	−154.4 (−153.2)	−164.1 (−151.1)	−162.1 (−159.5)	−157.0
Φ_4	−93.3	−93.9	−95.0	−84.2	−69.1	−75.7	−81.0	−76.5	−75.2	−89.2	−76.8	−92.7	−90.9	−75.4	−69.8 (−74.0)	−63.4 (−78.1)	−62.1 (−69.8)	−67.8
Ψ_4	−131.0	−132.9	−133.1	−124.8	−127.1	−119.6	−104.3	−117.5	−103.8	−107.9	−100.6	−102.3	−90.9	−85.6	−115.2 (−103.8)	−119.6 (−92.8)	−121.4 (−119.8)	−108.5
Φ_{H1}	−40.2	−39.4	−55.4	−61.3	−54.4	−68.9	−53.7	−66.3	−64.6	−57.5	−53.3	−59.9	−50.6	−57.3				
Ψ_{H1}	−73.9	−75.0	−46.2	−42.7	−52.9	−37.7	−59.6	−44.9	−33.8	−45.4	−46.6	−48.6	−41.4	−47.9				
Φ_{H2}	14.8	14.2	0.5	3.1	−5.3	17.7	−0.5	16.4	31.2	36.1	27.3	38.5	37.8	22.8				
Ψ_{H2}	23.9	22.7	55.8	53.7	42.2	44.1	46.0	37.3	47.8	37.4	42.4	34.7	31.1	39.3				
Φ_{H3}	−45.1	−48.2	−65.6	−73.1	−65.2	−64.5	−64.7	−54.7	−61.2	−70.8	−61.5	−67.0	−37.1	−47.1				
Ψ_{H3}	−30.7	−30.7	−50.2	−52.3	−57.7	−50.8	−55.5	−47.0	−52.0	−44.9	−54.8	−52.7	−34.1	−34.5				
Φ_{H4}	26.9	26.4	25.8	36.8	49.4	43.9	37.9	41.4	41.2	31.2	41.5	28.2	26.4	45.9				
Ψ_{H4}	−12.2	−14.2	−17.4	−9.6	−11.2	−4.6	12.9	−0.4	10.7	8.1	15.8	14.9	28.4	32.3				

[a] The X-ray structure of the second molecule in the asymmetric unit is in the parenthesis. [b] Values of experimentally determined Φ and Ψ torsional angles for the complex of antithrombin with pentasaccharide.[54] [c] X-ray experimental data for antithrombin in the pentasaccharide-bound intermediate state.[55] [d] Pentamer (Fondaparinux) anion from the cocrystal with antithrombin and coagulation factor Xa.[56]

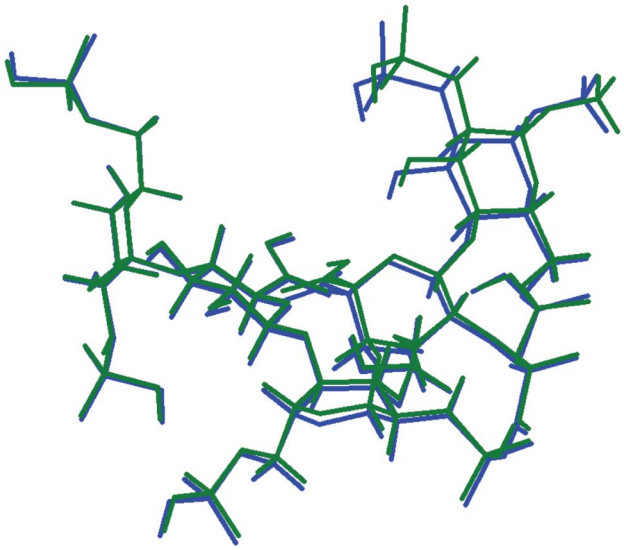

Fig. 2 Molecular superimposition of the Pentamer(D–E–F–G–H)···K^+ complex (green) and in water optimized Pentamer(D–E–F–G–H)···K^+ system (blue). For simplicity potassium cations are omitted.

their interactions with antithrombin. The overall structure of the pentasaccharide-M_{10} complexes (M = Li^+, Na^+, K^+, Mg^{2+} and Ca^{2+}) is somewhat bent (Fig. 4), and the hydroxyl groups of

Table 6 The Becke3LYP/6-31G(d) solvent stability (CPCM) of the metal complexes of oligomers of heparin investigated

Complex	ΔE, kJ mol^{-1}	Gas-phase dipole moment, Debye (D)
Dimer(D–E)···3Li^+	−321.34	12.25
Dimer(D–E)···3Na^+	−360.47	15.85
Dimer(D–E)···3 K^+	−339.89	19.09
Dimer(D–E)···3Mg^{2+}	−1840.46	25.41
Dimer(D–E)···3Ca^{2+}	−1967.80	27.95
Dimer(E–F)···4Li^+	−316.77	12.95
Dimer(E–F)···4Na^+	−352.33	11.27
Dimer(E–F)···4 K^+	−237.84	10.86
Dimer(E–F)···4Mg^{2+}	−2946.62	31.95
Dimer(E–F)···4Ca^{2+}	−2865.44	18.35
Dimer(F–G)···5Li^+	−506.69	10.85
Dimer(F–G)···5Na^+	−473.22	15.61
Dimer(F–G)···5 K^+	−422.70	11.05
Dimer(F–G)···5Mg^{2+}	−3891.42	29.53
Dimer(F–G)···5Ca^{2+}	−3923.37	30.61
Dimer(G–H)···4Li^+	−383.56	19.31
Dimer(G–H)···4Na^+	−359.60	7.66
Dimer(G–H)···4 K^+	−325.23	18.03
Dimer(G–H)···4Mg^{2+}	−2797.91	37.82
Dimer(G–H)···4Ca^{2+}	−2802.81	38.40
Pentamer(D–E–F–G–H)···10Li^+	−704.28	14.21
Pentamer(D–E–F–G–H)···10Na^+	−774.25	17.89
Pentamer(D–E–F–G–H)···10 K^+	−704.46	22.39
Pentamer(D–E–F–G–H)···10Mg^{2+}	−10113.88	38.62
Pentamer(D–E–F–G–H)···10Ca^{2+}	−10022.32	44.89
D–E (anion)	−1233.69	11.65
E–F (anion)	−1963.94	9.89
F–G (anion)	−2867.93	4.18
G–H (anion)	−1977.25	13.03
D–E–F–G–H (anion)		8.08

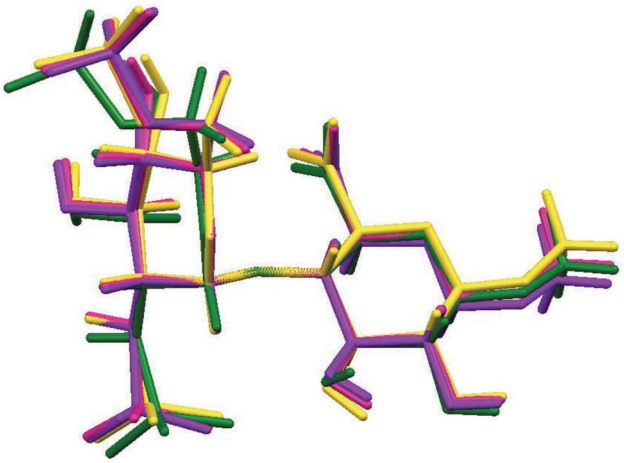

Fig. 3 Molecular superimposition of the dimer(D–E)···M^{n+} (Li^+ – rose, Na^+ – yellow, K^+ – violet, and Ca^{2+} – green) complexes. For simplicity cations are omitted.

the D, E, F, and H units are involved in intramolecular hydrogen bonds of the O–H···O type.

Structure of glycosidic linkage

For the definition of the torsion angles of the glycoside bonds, we use the recommendations and symbols for nomenclature proposed by the IUPAC.[48] The relative orientation of a disaccharide is described by two torsional angles at the glycoside linkage, which are denoted Φ and Ψ. For a (1 → 4) linkage, the definitions of these torsional angles are as follows: Φ = O(5)–C(1)–O(1)–C(4′) or Φ_H = H(1)–C(1)–O(1)–C(4′); Ψ = C(1)–O(1)–C(4′)–C(5′) or Ψ_H = C(1)–O(1)–C(4′)–H(4′). The bond angle τ = C–O–C and the bond lengths C(1)–O and O–C(4′) characterize the glycoside bonds in disaccharides. The optimized glycoside bond lengths, bond angle and torsional angles of the fully optimized D–E, E–F, F–G and G–H dimers are given in Tables 1–4. The monosaccharide units in a simple disaccharide are free to rotate about the inter-unit glycoside bonds. However, glycosaminoglycans contain bulky *O*-sulfate,

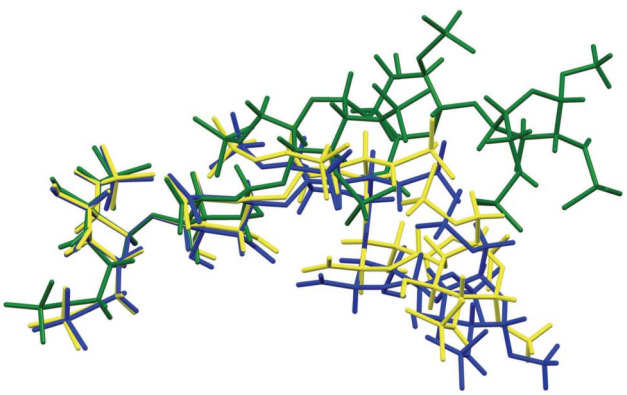

Fig. 4 Molecular superimposition of the pentamer(D–E–F–G–H)M^{n+} (Na^+ – yellow, K^+ – blue, and Ca^{2+} – green) complexes. For simplicity cations are omitted.

N-sulfate and carboxylate substituents at the C(2) and C(5′) carbon atoms. Hydrogen bonds between the constituent monosaccharide structural units form thermodynamically stable structures for only certain combinations of Φ and Ψ.[14] From a practical perspective, therapeutically important glycosaminoglycan drugs based on heparin are prepared as salts of alkali metal ions. The molecular structures of the isolated metal complexes of these dimers are determined by multiple coordinate bonds between metal cations and oxygen atoms in the negatively charged sulfate, carboxyl and hydroxyl groups. These specific interactions are responsible for the unique overall shapes of the individual complexes (Fig. 1A–4A, ESI†) and are manifested by the computed values of the structural parameters of the glycoside linkages. For the glycosidic bond angle τ = C–O–C, most X-ray data for simple disaccharide derivatives have a narrow distribution of values in the range $116^\circ \pm 2^\circ$ (for a review see[49,50]). The calculated glycosidic bond angles in the free acids of these dimers[14] are in the range of approximately 115°–117° and correspond well to the experimentally observed data for disaccharide structures. The glycosidic bond angles in the metal complexes of the D–E and F–G dimers of heparin have higher values, 120° –122°. A much larger range (108°–117°) of valence bond angles was found for the metal complexes of the dimers, (E–F)·M_4 and (G–H)·M_4, M = Li^+, Na^+, K^+, Mg^{2+} and Ca^{2+} (Tables 1–4). Computed bond lengths for glycosidic bonds C(1)–O and O–C(4′) are not the same and strongly depend on the mode of metal coordination in the dimer. Magnesium and calcium cations in the dimers, (E–F)·M_4 and (G–H)·M_4, M = Mg^{2+} and Ca^{2+}, directly coordinate with the oxygen atom of the glycosidic bond (Fig. 2A and 4A, ESI†). The polarizing effect of these dications on this bond increases the lengths of the C(1)–O and O–C(4′) bonds compared to the corresponding free acids.[14] Thus, the C(1)–O and O–C(4′) glycosidic bonds in these metal complexes are approximately 0.05–0.15 Å longer, Tables 2 and 4, than the typical values for this bond (approximately 1.42 Å) in disaccharides.[50]

The equilibrium structures of the Li^+, Na^+, K^+, Mg^{2+} and Ca^{2+} salts of the D–E, E–F, F–G and G–H dimers in their isolated states are determined by cation coordination with the sulfate, carboxyl and hydroxyl (hydroxymethyl) groups. These specific interactions produce the unique shapes of the individual dimeric complexes (Fig. 1A–4A, ESI†) and are manifested by the computed values of the Φ and Ψ torsional angles of the glycosidic linkages. Values of these angles for individual dimers differ considerably (Tables 1–4). The effect of water on the geometry of these dimeric complexes was examined using the CPCM solvation method. Optimal glycosidic angles of solvated species differ from those computed for isolated complexes by approximately 10–40° (Tables 1–4). Inter-ring orientations in these dimers are significantly influenced by the metal cation coordination and ionization.[12,14] Owing to the fact that the solute – solvent interactions are in general much smaller than the intramolecular forces, one may expect that geometrical parameters (such as torsion angles) with relative small force constants can cause substantial changes of the permanent electric moments, important solvent effects can appear on these parameters. However, appreciable changes of torsion angles after geometry optimization in solution were observed for Na(I) salt of dimer E–F and Mg(II) salt of dimer G–H, only. It is interesting to note that also an explicit consideration of water molecules on the conformational structure of sodium and calcium salts of heparin disaccharide containing induronic acid residue showed that solvent did not produce an appreciable change in torsion angles of the system studied.[16] However, inter–ring orientations in these dimers are significantly influenced by the metal cation coordination and ionization.[12,14]

Because the metal complexes of these dimers have not been prepared, experimental geometries based on X-ray measurements are not available, and our computed data cannot be directly compared and discussed with experiment results. However, similar experimental structural data are available for more complex penta- and hexasaccharide heparin structures in protein complexes. Although the pentasaccharide Fondaparinux is a chemically well-characterized drug,[51,52] no single crystals suitable for X-ray diffraction studies are available, and its solid state structure is unknown. In the absence of experimental data for Fondaparinux, the geometry of this pentamer can be compared with X-ray structural data for complexes of synthetic pentasaccharides[53] with therapeutically relevant antithrombin,[54] X-ray experimental data for complexes of Idraparinux with antithrombin in the heparin-bound intermediate state[55] and/or the synthetic version of Fondaparinux in complexes with antithrombin and coagulation factor Xa.[56] Published co-crystal structures of pentasaccharides and proteins highlight the ionic interactions between specific anionic sulfate and carboxyl moieties of pentasaccharides with the basic cationic amino acid residues at the binding sites in proteins.[47,54–56] However, ionic contacts alone are not sufficient to explain the optimal structural fit of a pentasaccharide to the binding site of a protein. Interactions between the pentasaccharide and the protein induce conformational changes in the pentasaccharide, which are manifested as changes in the glycosidic torsional angles. This behavior is apparent in the biologically active conformations of pentasaccharides in co-crystals with different proteins and/or environments.[54–56] In the experimentally determined structures, the bound pentasaccharide and antithrombin receptor (pdb files 1AZX, 1E03, and 1NQ9) are in close proximity (Table 5). In complexes of antithrombin and coagulation factor Xa, the spatial orientation of the bound pentasaccharide is completely different (pdb file 2GD4), Table 5. A comparison of torsional glycosidic bonds for these pentasaccharides shows that the substitution pattern of the pentasaccharide and the biological environment produces different biologically active conformations of individual pentasaccharides. Langeslay *et al.* examined heparin oligosaccharides using NMR experiments and molecular dynamics calculations.[57] They showed that the intramolecular hydrogen bond between the internal glucosamine sulfamate NH and the adjacent 3-*O*-sulfo group stabilizes the conformation at the F structural unit of Fondaparinux sodium. This kind of interaction is also observed in the anionic structure of Fondaparinux anion calculated by us with an optimal hydrogen bond distance of about 2.6 Å. The values of the glycosidic angles of the pentamer (D–E–F–G–H)·M_{10}, M = Li^+, Na^+, K^+, Mg^{2+} and Ca^{2+} complexes and the computed values for the bond angles of the free acid[14] are listed in

Table 5. The equilibrium structures of the pentamer-metal complexes are determined by the multidentate coordination of the negatively charged sulfate and carboxylate groups with the metal cations Li^+, Na^+, K^+, Mg^{2+} and Ca^{2+}. Individual cations have different effects on the conformational structure of the pentamer. The largest changes in the torsional bond angles are observed for glycosidic bonds connecting the F–G and G–H structural units (Table 5) coordinated with bivalent metal cations Mg^{2+} and Ca^{2+}, respectively. The change in 3D structure of the pentasaccharide upon metal complex formation is not regular, and individual complexes are configured differently, *e.g.*, Li^+, Na^+, and K^+ complexes form more bent structures (Fig. 4). The solvation of the individual pentameric salts slightly increases the $M^{n+}\cdots O$ (M = Li^+, Na^+, K^+, Mg^{2+} and Ca^{2+}) distances and causes appreciable changes in the corresponding torsional bond angles (Tab. 5). The displacement of the Na^+ ions from their binding sites in the sodium salt of Fondaparinux causes appreciable changes in the conformation of the corresponding anion.[13] Upon dissociation, large changes are observed in the positions of the sulfate groups and the conformation across the glycosidic bonds.[13,14] The same effect is observed for other metal complexes studied in the present work. Sodium Fondaparinux is an off-white powder, freely soluble in water, and it is administered parenterally. The biologically active form of Fondaparinux is an anion. It is reasonable to compare the computed anionic structure with the available experimental data[56] for Fondaparinux bound to proteins (Table 5). Computed and experimental structures of Fondaparinux were determined in different molecular environments, and only general structural motifs are compared. Some computed torsional angles for unbound Fondaparinux (*e.g.*, angles Ψ_1, Φ_2, Ψ_3 and Φ_4) correspond well to the structure of this drug bound to the antithrombin receptor in the antithrombin factor Xa – Fondaparinux complex.[56] However, in general, the biologically active conformation and the structure of unbound Fondaparinux are very different (Table 5). The molecular structure of heparin oligosaccharides is an object of several experimental and theoretical examinations.[58–68] The majority of these were not analysed for this study of Fondaparinux because they involve different heparin oligomeric structural units and/or synthetic heparin derivatives.

Gas phase metal affinities

Table 7 contains computed total interaction energies (metal affinities) of the dimer- and pentameric-M^{n+} (M^{n+} = Li^+, Na^+, K^+, Mg^{2+} and Ca^{2+}) complexes and metal affinities per cation. No corrections for basis set superposition errors (BSSE) were incorporated in the results because the B3LYP/6-311+G(d,p) values for simpler metal complexes of organic bases are close to the CBS–QB3 results with an average absolute deviation of approximately 20 kJ mol^{-1}.[42] The CBS–QB3 model chemistry represents a high-level calculation with a very large basis set. Thus, the basis set used here is adequate to reduce the basis set superposition error effects. The computed interaction energies represent values for dissociation energies of metal ions from several binding sites in the dimers and pentamer studied in this work. Because most of the ions and the basic centers in these glycosaminoglycans are multiply coordinated,

Table 7 B3LYP/6-311+G(d,p) calculated interaction energies ΔE (kJ mol^{-1}) of the ion-dimers and ion-pentamer systems

Complex	ΔE, total	ΔE, per M^{n+}
Dimer(D–E)$\cdots 3Li^+$	−2467.72	−822.57
Dimer(D–E)$\cdots 3Na^+$	−2155.53	−718.51
Dimer(D–E)$\cdots 3\ K^+$	−1926.49	−642.16
Dimer(D–E)$\cdots 3Mg^{2+}$	−4630.02	−1543.34
Dimer(D–E)$\cdots 3Ca^{2+}$	−3933.06	−1311.02
Dimer(E–F)$\cdots 4Li^+$	−3813.91	−953.48
Dimer(E–F)$\cdots 4Na^+$	−3374.61	−843.65
Dimer(E–F)$\cdots 4\ K^+$	−3131.42	−782.86
Dimer(E–F)$\cdots 4Mg^{2+}$	−6291.98	−1572.99
Dimer(E–F)$\cdots 4Ca^{2+}$	−5311.21	−1327.80
Dimer(F–G)$\cdots 5Li^+$	−5037.79	−1007.56
Dimer(F–G)$\cdots 5Na^+$	−4594.32	−918.86
Dimer(F–G)$\cdots 5\ K^+$	−4248.23	−849.65
Dimer(F–G)$\cdots 5Mg^{2+}$	−7704.26	−1540.85
Dimer(F–G)$\cdots 5Ca^{2+}$	−6727.63	−1345.52
Dimer(G–H)$\cdots 4Li^+$	−3752.98	−938.24
Dimer(G–H)$\cdots 4Na^+$	−3390.83	−847.71
Dimer(G–H)$\cdots 4\ K^+$	−3094.08	−773.52
Dimer(G–H)$\cdots 4Mg^{2+}$	−6243.25	−1573.31
Dimer(G–H)$\cdots 4Ca^{2+}$	−5388.83	−1347.21
Pentamer(D–E–F–G–H)$\cdots 10Li^+$	−13323.24[a]	−1332.32[a]
Pentamer(D–E–F–G–H)$\cdots 10Na^+$	−12365.39[a]	−1236.37[a]
Pentamer(D–E–F–G–H)$\cdots 10\ K^+$	−11379.49[a]	−1137.95[a]
Pentamer(D–E–F–G–H)$\cdots 10Mg^{2+}$	−16398.60[a]	−1639.86[a]
Pentamer(D–E–F–G–H)$\cdots 10Ca^{2+}$	−13755.74[a]	−1375.57[a]

[a] B3LYP/6-31G(d) method.

the interaction energies are highly negative and span a broad energy interval from −1900 to −16000 kJ mol^{-1}. For alkali metal complexes, the calculated order of stability ($Li^+ > Na^+ > K^+$) follows the order expected on the basis of their ionic radii[43,44]. The Mg^{2+} complexes are always more stable that the Ca^{2+} complexes, which is consistent with their ionic sizes (Mg^{2+} (0.65 Å), Ca^{2+} (1.0 Å)).[43,44]

The primary applications of the alkali salts of heparin and its simpler synthetic products (Fondaparinux, Idraparinux) are in the pharmaceutical industry. The alkali cations Mg^{2+} and Ca^{2+} interact strongly with anionic centers in oligomeric structures (Table 7). In some cases, these cations interact with native heparin and extracellular proteins.[22,69,70] Because there is a formal charge of +2, it is likely that Mg^{2+} and Ca^{2+} cations participate in networks with the anionic residues of proteins and/or participate in territorial interactions.[20]

It was shown experimentally[71–74] that heparin – protein interactions are modified through divalent ions such as calcium or magnesium. E.g. Ca^{2+} moderates the anticoagulant activity of heparin,[73] and it potentiates the acceleration by heparin of thrombin inhibition by antithrombin III and the anti-Factor Xa activity of heparin.[74] It is probable that calcium dication, owing of its larger ionic size is able to interfere with heparin and protein binding sites more effectively. Besides electrostatic effects also some site-specific contribution to the bonding of Ca^{2+} will take part. Mg^{2+} cation coordinates to the anionic groups of Fondaparinux more strongly. Its shorter ionic radii leads to stronger electrostatic effect and in addition to higher interaction energies (Table 7). The hard nature of the

Mg^{2+} ion and shorter ionic radii in comparison with the Ca^{2+} cation may restrict its coordination to the binding sites of the heparin – protein complex and/or water molecules.

The computed total alkali and alkaline metal cation affinities result from the dissociation of several metal cations from their interaction sites. For a more exact characterization of the contributions of single counterions to the total interaction energy, we calculated metal affinities per cation. Theoretical values of the metal affinities per M^{n+} (M^{n+} = Li^+, Na^+, K^+, Mg^{2+} and Ca^{2+}) cation calculated for individual heparin oligomers differ for various dimeric and pentameric structures. Interaction energies, ΔE, per M^{n+} gradually increase with the number of anionic centers, and a synergistic effect is observed, *e.g.*, ΔE per M^{n+} is approximately −800, −950, −1000 and −1300 kJ mol^{-1} for 3, 4, 5 and 10 coordination centers, respectively, in Li^+ complexes (Table 7).

Conclusions

Quantum chemical calculations at the density functional level have shown that metal ions produce conformational changes in D–E, E–F, F–G and G–H dimers. Counter ions induce a considerable conformational contraction in the complex pentasaccharide Fondaparinux. Values of glycosidic torsion angles for individual dimers and counterions differ considerably. The effect of water on the geometry of these dimeric complexes was examined using the CPCM solvation method. Optimal glycosidic angles of solvated species differ from those computed for isolated complexes by approximately 10–40°. Inter-ring orientations in these dimers are significantly influenced by metal cation coordination, ionization and/or solvent effects. The displacement of the counterions from their binding sites in the salts of Fondaparinux results in appreciable changes of the overall conformation of the corresponding anion. Upon dissociation, large changes are observed in the positions of the sulfate groups and the conformations of the glycosidic bonds. The interaction energies of the dimeric and pentameric-M^{n+} (M^{n+} = Li^+, Na^+, K^+, Mg^{2+} and Ca^{2+}) complexes are highly negative and span a broad energy range from −1900 to −16 000 kJ mol^{-1}. The charge of the ion, the number of metal ion adducts and the ionic radii of the counterions are factors in counterion-induced conformational change of the dimeric and pentameric heparin structures studied here. This work yields quantities that may be inaccessible or complement experimental results, and this is the first quantum chemical approach to the determination of gas and solvated phase 3D structures of complexes of dimeric and pentameric heparin units with M^{n+} (M^{n+} = Li^+, Na^+, K^+, Mg^{2+} and Ca^{2+}) counterions.

Acknowledgements

This work has been supported by The European Union HPC-Europa Transnational Access Program under the Project HPC-Europa2 (Project No 863) at SARA Amsterdam. The authors acknowledge with thanks the Stichting Academisch Rekencentrum Amsterdam (SARA) for the use of its resources and for excellent support. M.R. thanks the Department of Theoretical Chemistry, Zernike Institute for Advanced Materials, University of Groningen, for its hospitality during his study stay in Groningen.

References

1 J. Xie, S. Nurugesan and R. J. Linhard, Physiological, Pathophysiological and Therapeutic Roles of Heparin/Heparan Sulfate, H. G. Garg, M. K. Cowman, C. A. Hales, ed. in *Carbohydrate Chemistry, Biology and Medical Applications*, Chapter 10, 227–251, Elsevier, Oxford , UK, 2008.
2 U. R. Desai, *Med. Res. Rev.*, 2004, **24**, 151–181.
3 R. J. Linhardt, *J. Med. Chem.*, 2003, **46**, 2551–2564.
4 J. Liu and S. C. Thorp, *Med. Res. Rev.*, 2002, **22**, 1–25.
5 D. L. Rabenstein, *Nat. Prod. Rep.*, 2002, **19**, 312–331.
6 D. A. Lane and U. Lindahl (ed.). *Heparin – Chemical and Biological Properties*, CRC Press, Boca Raton, FL, 1989.
7 B. Casu and U. Lindahl, *Adv. Carbohydr. Chem. Biochem.*, 2001, **57**, 159–206.
8 H.–M. Wang, D. Loganathan and R. J. Linhardt, *Biochem. J.*, 1991, **278**, 689–695.
9 M. Remko and C. W. von der Lieth, *J. Chem. Inf. Model.*, 2006, **46**, 1194–1200.
10 I. Capila and R. J. Linhardt, *Angew. Chem., Int. Ed.*, 2002, **41**, 390–412.
11 M. Petitou and C. A. A. van Boeckel, *Angew. Chem., Int. Ed.*, 2004, **43**, 3118–3133.
12 M. Remko and C. W. Von der Lieth, *J. Chem. Inf. Model.*, 2006, **46**, 1687–16.
13 M. Remko and C. W. Von der Lieth, *J. Phys. Chem. A*, 2007, **111**, 13484–13491.
14 M. Remko, P. Th. Van Duijnen and R. Broer, *Struct. Chem.*, 2010, **21**, 965–976.
15 M. Remko, M. Swart and F. M. Bickelhaupt, *J. Phys. Chem. A*, 2006, **110**, 1960–1967.
16 M. Hricovíni, *J. Phys. Chem. B*, 2011, **115**, 1503–1511.
17 L. B. Jaques, *Pharmacol. Rev.*, 1980, **31**, 99–166.
18 B. Lages and S. S. Stivala, *Biopolymers*, 1973, **12**, 127–143.
19 L. Herwats, P. Laszlo and P. Genard, *Nouv. J. Chem.*, 1977, **1**, 173–176.
20 F. Chevalier, J. Angulo, R. Lucas, P. M. Nieto and M. Martín-Lomas, *Eur. J. Org. Chem.*, 2002, 2367–2376.
21 T. R. Rudd, S. E. Guimond, M. A. Skidmore, L. Duchesne, M. Guerrini, G. Torri, C. Cosentino, A. Brown, D. T. Clarke, J. E. Turnbull, D. G. Yates and E. A. Yates, *Glycobiology*, 2007, **17**, 983–993.
22 Y. Seo, M. R. Schenauer and J. A. Learly, *Int. J. Mass Spectrom.*, 2011, **303**, 191–198.
23 D. L. Rabenstein, J. M. Robert and J. Peng, *Carbohydr. Res.*, 1995, **278**, 239–256.
24 J. Wang and D. L. Rabenstein, *Biochim. Biophys. Acta 2009*, 1790, 1689–1697.
25 M. J. Frisch, G. W. Trucks, H. B. Schlegel, G. E. Scuseria, M. A. Robb, J. R. Cheeseman, G. Scalmani, V. Barone, B. Mennucci, G. A. Petersson, H. Nakatsuji, M. Caricato, X. Li, H. P. Hratchian, A. F. Izmaylov, J. Bloino, G. Zheng, J.

L. Sonnenberg, M. Hada, M. Ehara, K. Toyota, R. Fukuda, J. Hasegawa, M. Ishida, T. Nakajima, Y. Honda, O. Kitao, H. Nakai, T. Vreven, J. A. Montgomery Jr., J. E. Peralta, F. Ogliaro, M. Bearpark, J. J. Heyd, E. Brothers, K. N. Kudin, V. N. Staroverov, R. Kobayashi, J. Normand, K. Raghavachari, A. Rendell, J. C. Burant, S. S. Iyengar, J. Tomasi, M. Cossi, N. Rega, J. M. Millam, M. Klene, J. E. Knox, J. B. Cross, V. Bakken, C. Adamo, J. Jaramillo, R. Gomperts, R. E. Stratmann, O. Yazyev, A. J. Austin, R. Cammi, C. Pomelli, J. W. Ochterski, R. L. Martin, K. Morokuma, V. G. Zakrzewski, G. A. Voth, P. Salvador, J. J. Dannenberg, S. Dapprich, A. D. Daniels, Ö. Farkas, J. B. Foresman, J. V. Ortiz, J. Cioslowski and D. J. Fox*Gaussian 09, Version 9.0*, Gaussian Inc., Wallingford, CT, 2011.

26 R. G. Parr and W. Wang, *Density-Functional Theory of Atoms and Molecules*, Oxford University Press, New York, 1994.

27 R. Neumann, R. H. Nobes and N. C. Handy, *Mol. Phys.*, 1996, **87**, 1–36.

28 F. M. Bickelhaupt and E. J. Baerends, In *Rev. Comput. Chem.*, K. B. Lipkowitz, D. B. Boyd, (ed.) Wiley-VCH, New York, 2000,, 15, pp 1–86.

29 A. D. Becke, *Phys. Rev.*, 1988, **A38**, 3098–3100.

30 A. D. Becke, *J. Chem. Phys.*, 1993, **98**, 5648–5652.

31 C. Lee, W. Yang and R. G. Parr, *Phys. Rev.*, 1988, **B37**, 785–789.

32 W. J. Hehre, L. Radom, P. V. R. Schleyer and J. A. Pople, *Ab Initio Molecular Orbital Theory*, Wiley, New York, 1986.

33 S. Miertuš, E. Scrocco and J. Tomasi, *Chem. Phys.*, 1981, **55**, 117–129.

34 A. Klamt and G. Schűűman, *J. Chem. Soc., Perkin Trans. 2*, 1993, 799–805.

35 V. Barone and M. Cossi, *J. Phys. Chem. A*, 1998, **102**, 1995–2001.

36 M. Cossi, N. Rega, G. Scalmani and V. Barone, *J. Comput. Chem.*, 2003, **24**, 669–681.

37 M. Remko and M. Hricovíni, *Struct. Chem.*, 2007, **18**, 537–547.

38 Ch. J. Barden and H. F. Schaefer III, Accuracy and applicability of quantum chemical methods in computational medicinal chemistry. in: P. Bulltinck, J. P. Tollenaere, H. de Winter (eds), *Computational medicinal chemistry for drug discovery*, Marcel Dekker, Inc, New York, pp 133–150.

39 M. Remko, A. Boháč and L. Kováčiková, *Struct. Chem.*, 2011, **22**, 635–648.

40 Y. Takano and K. N. Houg, *J. Chem. Theory Comput.*, 2005, **1**, 70–77.

41 C. C. Pye and T. Ziegler, *Theor. Chem. Acc.*, 1999, **101**, 396–408.

42 M. Remko and B. M. Rode, *J. Phys. Chem. A*, 2006, **110**, 1960–1967.

43 J. J. R. Fraústo da Silva and R. J. P. Williams, *The Biological Chemistry of the Elements*, Claredon Press, Oxford, 1991.

44 K. B. Harvey and G. B. Porter, *Introduction to Physical Inorganic Chemistry*, Addison Wesley Publ. Comp. Inc., London, 1963.

45 M. Remko, P. Th. van Duijnen and C. W. von der Lieth, *THEOCHEM*, 2007, **814**, 119–125.

46 K. J. Belzar, T. R. Dafforn, M. Petitou and R. W. Carrell, *J. Biol. Chem.*, 2000, **275**, 8733–8741.

47 M. Remko, P. Th. Van Duijnen and R. Broer, *RSC Adv.*, 2013, **3**, 1789–1796.

48 http://www.chem.qmul.ac.uk/iupac/2carb/.

49 S. Arnott and W. E. Scott, *J. C. S. Perkin II*, 1962, 324–335.

50 V. S. R. Rao, P. K. Qasba, P. V. Balaji and R. Chandrasekaran, *Conformation of Carbohydrates*, Harwood Academic Publishers, Amsterdam, 1998.

51 J. M. Walenga, J. Fareed, W. P. Jeske, F. X. Frapaise, R. L. Bick and M. M. Samama, *Turk J Haematol*, 2002, **19**, 137–150.

52 A. Manikowski, A. Kozioł and E. Czajkowska-Wojciechowska, *Carbohydr. Res.*, 2012, **361**, 155–161 and references cited therein.

53 J. Basten, G. Jaurand, B. Olde-Hanter, P. Duchaussoy, M. Petitou and C. A. A. van Boeckel, *Bioorg. Med. Chem. Lett.*, 1992, **2**, 905–910.

54 L. Jin, J. P. Abrahams, R. Skinner, M. Petitou, R. N. Pike and R. W. Carrell, *Proc. Natl. Acad. Sci. U. S. A.*, 1997, **94**, 14683–14688.

55 D. J. D. Johnson and J. A. Huntington, *Biochemistry*, 2003, **42**, 8712–8719.

56 D. J. D. Johnson, W. Li, T. E. Adams and J. A. Huntington, *EMBO J.*, 2006, **25**, 2029–2037.

57 D. J. Langeslay, R. P. Young, S. Beni, C. N. Beecher, L. J. Mueller and C. K. Larive, *Glycobiology*, 2012, **22**, 1173–1182.

58 A. Almond and J. K. Sheehan, *Glycobiology*, 2000, **10**, 329–338.

59 C. Landersjö and G. Widmalm, *Biopolymers*, 2002, **64**, 283–291.

60 H. Verli and J. A. Guimarães, *Carbohydr. Res.*, 2004, **339**, 281–290.

61 C. F. Becker, J. A. Guimarães and H. Verli, *Carbohydr. Res.*, 2005, **340**, 1499–1507.

62 A. K. Powell, E. A. Yates, D. G. Fering and J. E. Turnbull, *Glycobiology*, 2004, **14**, 17R–30R.

63 L. Jin, P. E. Barran, J. A. Deakin, M. Lyon and D. Uhrín, *Phys. Chem. Chem. Phys.*, 2005, **7**, 3464–3471.

64 Z. Zhang, S. A. McCallum, J. Xie, L. Nieto, F. Corzana, J. Jiménez-Barbero, M. Chen, J. Liu and R. J. Linhardt, *J. Am. Chem. Soc.*, 2008, **130**, 12998–13007.

65 L. Jin, M. Hricovíni, J. A. Deakin, M. Lyon and D. Uhrín, *Glycobiology*, 2009, **19**, 1185–1196.

66 S. Khan, J. Gor, B. Mulloy and S. J. Perkins, *J. Mol. Biol.*, 2010, **395**, 504–525.

67 S. A. Samsonov, J. Teyra and M. T. Pisabarro, *J. Comput.-Aided Mol. Des.*, 2011, **25**, 477–489.

68 M. Herczeg, L. Lázár, Z. Bereczky, K. E. Kövér, I. Timári, J. Kappelmayer, A. Lipták, S. Antus and A. Borbás, *Chem.–Eur. J.*, 2012, **18**, 10643–10652.

69 M. Kan, F. Wang, J. Xu, J. W. Crabb, J. Hou and W. L. McKeehan, *Science*, 1993, **259**, 1918–1921.

70 I. Capila, M. J. Hernáiz, Y. D. Mo, T. R. Mealy, B. Campos, J. R. Dedman, R. J. Linhardt and B. A. Seaton, *Structure*, 2001, **9**, 57–64.

71 F. Zhang, Y. Wu, Q. Ma, D. Hoppensteadt, J. Fareed and R. J. Linhardt, *Clin. Appl. Thromb./Hemostasis*, 2004, **10**, 249–257.

72 N. H. H. Heegaard, X. He and L. G. Blomberg, *Electrophoresis*, 2006, **27**, 2609–2615.

73 S. C. Alter and L. B. Schwartz, *Biochim. Biophys. Acta, Gen. Subj.*, 1989, **991**, 426–430.

74 T. W. Barrowcliffe and Y. LeShirley, *Thromb. Haemostas.*, 1988, **62**, 950–954.